Available online at www.sciencedirect.com
ScienceDirect
Journal of Solid State Chemistry 180 (2007) 2649–2654
JOURNAL OF SOLID STATE CHEMISTRY
www.elsevier.com/locate/jssc

Synthesis, Mo-valence state, thermal stability and thermoelectric properties of $SrMoO_{3-x}N_x$ ($x>1$) oxynitride perovskites

D. Logvinovich[a], R. Aguiar[b], R. Robert[a], M. Trottmann[a], S.G. Ebbinghaus[b], A. Reller[b], A. Weidenkaff[a,*]

[a]*Empa, Swiss Federal Laboratories for Materials Testing and Research, Solid State Chemistry and Catalysis, Ueberlandstr. 129, CH-8600 Duebendorf, Switzerland*
[b]*Universität Augsburg, Festkörperchemie, Institut für Physik, Universitätsstrasse 1, D-86159 Augsburg, Germany*

Received 15 March 2007; received in revised form 5 June 2007; accepted 20 June 2007
Available online 20 July 2007

Abstract

Oxynitrides of the general composition $SrMoO_{3-x}N_x$ ($x>1$) were synthesized by thermal ammonolysis of crystalline $SrMoO_4$. According to neutron and X-ray diffraction experiments, the materials crystallize in the cubic perovskite structure (space group $Pm\bar{3}m$). X-ray absorption spectroscopy (XAS) shows evidence of local distortions of the $Mo(O,N)_6$ octahedra. The oxidation states of Mo determined by X-ray absorption near edge structure (XANES) spectroscopy are slightly lower than that calculated from the oxygen/nitrogen(O/N) content. The disagreement arises from the higher covalence of the Mo–N bonding when compared to the Mo–O bonding (''chemical shift''). The electrical transport properties of the samples are strongly different from $SrMoO_3$. It was found that the conductivity of the samples decreases with increasing nitrogen content. The Seebeck coefficient values are up to three times higher than those of $SrMoO_3$.

Keywords: Oxynitride; Molybdate; XANES; Electronic properties

1. Introduction

Partial oxygen substitution by nitrogen in perovskite-type oxides of the general formula ABO_3 is an interesting method to change their physical properties [1,2]. Since N^{3-} has a higher negative charge than O^{2-}, nitrogen insertion into the oxygen sublattice formally leads to an increase of the *B*-site cation oxidation state, and consequently changes the charge carriers concentration. This method has been considered as an alternative to the cationic substitution to change transport properties of the p-type conducting $LaVO_3$ [1]. Similar to the Ba^{2+} and Sr^{2+} substituted $LaVO_3$, the synthesized oxynitrides of general formula $LaVO_{3-x}N_x$ ($x<0.53$) show an increased electrical conductivity compared to that of $LaVO_3$. While the conductivity of Sr^{2+} and Ba^{2+} containing samples changes from semiconducting to metallic when increasing the substitution level of La^{3+} [3,4], all the oxynitride samples remain semiconducting. Moreover, a decrease of the electrical conductivity with increasing nitrogen content was measured for the oxynitride samples with $x>0.53$. Thus, changing the nitrogen content can lead to a dramatic change of the physical properties of oxynitrides.

Another example in which oxygen substitution for nitrogen leads to materials with modified physical properties is the $SrMoO_{3-x}N_x$ system. Up to now, only studies on samples with $x\leqslant 0.5$ ($SrMoO_{2.6}N_{0.4}$ and $SrMoO_{2.5}N_{0.5}$) have been described in the literature [5,6]. Both neutron and X-ray diffraction (XRD) confirm no deviation from the cubic symmetry (space group $Pm\bar{3}m$) for these compositions. Their electronic conductivity was several orders of magnitude lower than that of $SrMoO_3$ [7].

Herein we report the synthesis procedure for higher level substituted oxynitrides of the composition $SrMoO_{3-x}N_x$, in particular of those with $x>1$. Furthermore, their

*Corresponding author.
E-mail address: anke.weidenkaff@empa.ch (A. Weidenkaff).

0022-4596/$ - see front matter © 2007 Elsevier Inc. All rights reserved.
doi:10.1016/j.jssc.2007.06.035

crystallographic structure and physical properties are investigated in detail. The results obtained by neutron diffraction (ND), XRD, X-ray absorption near edge spectroscopy, Seebeck coefficient and electrical conductivity measurements are presented.

2. Experimental

A total of 0.04 mol MoO_3 (JMC, Specpure) was dissolved in minimal amount of NH_3 (aq, 25%) and precipitated with 100 mL of an aqueous solution of $Sr(NO_3)_2$ (Merck, >99%) with the concentration of 0.4 mol/L. The precipitate was washed with distilled water, dried and annealed at 1073 K for 4 h to form phase pure, well crystalline $SrMoO_4$ as confirmed by XRD (Fig. 1A).

$SrMoO_3$ was prepared by reduction of 1 g freshly synthesized $SrMoO_4$ at $T = 1373$ K with forming gas (5% H_2/95% N_2, 99.999% purity, Pangas). A gas flow of 300 mL/min was applied. The reduction was completed in 5 h. The prepared material was of a purple-red color. Its phase purity was confirmed by XRD (Fig. 1B). The lattice parameter refined from the XRD data, $a = 3.9752(1)$ Å, is in perfect agreement with the previously reported value of 3.9751(3) Å for the sample with anionic stoichiometry equal to 3 [7]. When stored at ambient conditions $SrMoO_3$ transforms slowly to $SrMoO_4$. The presence of moisture promotes a faster $SrMoO_4$ formation. Therefore, in between handlings the material was kept in a desiccator.

The thermal ammonolysis of $SrMoO_4$ was performed in a rotating cavity reactor described elsewhere [8]. A total of 2.25 g of the $SrMoO_4$ powder was ammonolysed at

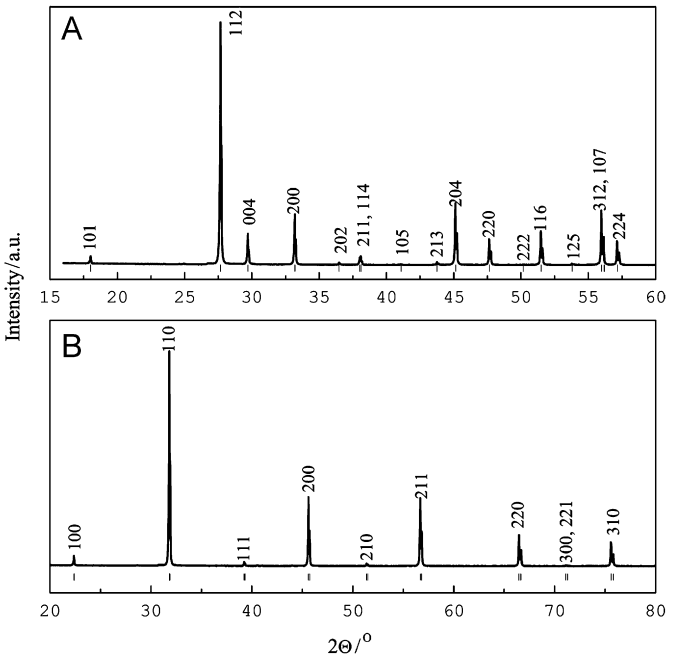

Fig. 1. XRD patterns confirming the phase purity of: (A) $SrMoO_4$ after annealing at 1073 K for 4 h. Space group: $I41/a$. The reflections are assigned according to the pdf entry 01-085-0809. (B) $SrMoO_3$ ($Pm\bar{3}m$, $a = 3.9752(1)$ Å) obtained by the reduction of $SrMoO_4$.

$T = 1073$ K under ammonia (PanGas, >99.98%) flow of 150 mL/min. The synthesis temperature was reached with a heating rate of 10 K/min. After the reaction, the furnace was cooled down to room temperature with a cooling rate of 10 K/min under flowing ammonia. Three samples with different oxygen/nitrogen (O/N) content were obtained after 11, 48 and 72 h of the ammonolysis.

The cationic composition was studied by energy dispersive X-ray spectrometry (EDXS-Link Pentafet 5947, from Oxford Microanalysis group). The O/N content of the different samples was measured by the hotgas-extraction method using a LECO TC500 analyzer. Silicon nitride and silicon oxide were used as calibration standards for nitrogen and oxygen, respectively.

Structure and phase purity of the obtained oxynitrides were investigated by X-ray diffraction using a Phillips X'Pert PRO MPD Θ–Θ system equipped with a linear detector X'Celerator. Lattice parameters were obtained from Rietveld refinements of the XRD data.

ND data were recorded at the high resolution powder diffractometer for thermal neutrons (HRPT) [9] located at the Swiss Spallation Neutron Source (SINQ) of the Paul Scherrer Institute in Switzerland as well as at the SPODI diffractometer of the FRM2 in Garching, Germany. Samples were placed in cylindrical vanadium cans with 8 mm diameter. The measurements were performed with a neutron wavelength $\lambda = 1.54842$ Å in the angular range of 2–152° with a step size of 0.05°. The background was fitted with a 6-coefficients polynomial function. The peak shape was modeled using a Tompson–Cox–Hastings pseudo Voigt function. Structure refinements were done using Fullprof [10].

X-ray absorption near edge structure (XANES) measurements at the Mo*K*-edge were performed at the beamline CEMO at the Hamburger Synchrotron Radiation Laboratory, HASYLAB. Data were collected in transmission mode. The energy scale was calibrated from the first inflection point in the *K*-edge of Mo metal (19.999 keV), which was measured simultaneously as reference. The beamline was equipped with a double-crystal fixed exit monochromator with Si(311) crystal pairs. Signal intensities where detuned to 40% of their maximum levels to minimize contributions of higher harmonics. Spectra were acquired in 2 eV increments for the pre-edge region (19.80–19.98 keV) and 0.20 eV near the edge (19.98–20.03 keV). $SrMoO_3$ and $SrMoO_4$ were measured as standards for Mo^{4+} and Mo^{6+} respectively. For data analysis the software package WinXAS v3.1 was used [11].

The electrical transport measurements were performed on bars with dimensions of 1.65 mm × 5–10 mm × 1 mm. The bars were obtained by applying an uniaxial pressure of 10 bar followed by a cold isostatic pressing at 2000 bar. The bars were sintered at $T = 1073$ K for half an hour under flowing ammonia. This short sintering time has no significant influence on the O/N content and purity of the samples as verified by hotgas extraction and X-ray powder diffraction. The measured density of the obtained ceramics

varied from 74% to 89% of the theoretical density. Electrical conductivity (DC four-probe method) and Seebeck coefficient were measured simultaneously as a function of temperature in the temperature range of $340\,K < T < 950\,K$ using the RZ2001i measurement system from Ozawa science, Japan. For the measurements Pt-contacts were used.

3. Results and discussion

According to the XRD results (Fig. 2), a perovskite-type single-phase oxynitride is already obtained after 11 h of ammonolysis at $T = 1073\,K$, whereas the formation of Mo_2N impurity phase was observed at higher temperatures.

The samples are of a dark-blue color. Similar to $SrMoO_3$ they are sensitive to the storing conditions. In particular, in contact with moisture they evolve ammonia and transform into $SrMoO_4$ within a period of a few months. Since the samples may also react with oxygen they were stored in dry N_2 after the synthesis.

The O/N content measured by hotgas extraction corresponds to the compositions $SrMoO_{1.95(5)}N_{1.05(5)}$, $SrMoO_{1.81(5)}N_{1.19(5)}$ and $SrMoO_{1.73(5)}N_{1.27(5)}$ for the compounds obtained after 11, 48 and 72 h of ammonolysis, respectively. Hence, the nitrogen content of our samples is more than twice higher than reported before [5,6]. The measured O/N content corresponds to a mixed oxidation state between $+5/+6$ for Mo. EDX reveal an average Sr:Mo ratio of all oxide and oxynitride samples equal to 0.98(1):1.02(2). Thus, within this method mistake (about 3%) the obtained ratio is identical with the ideal ratio 1:1.

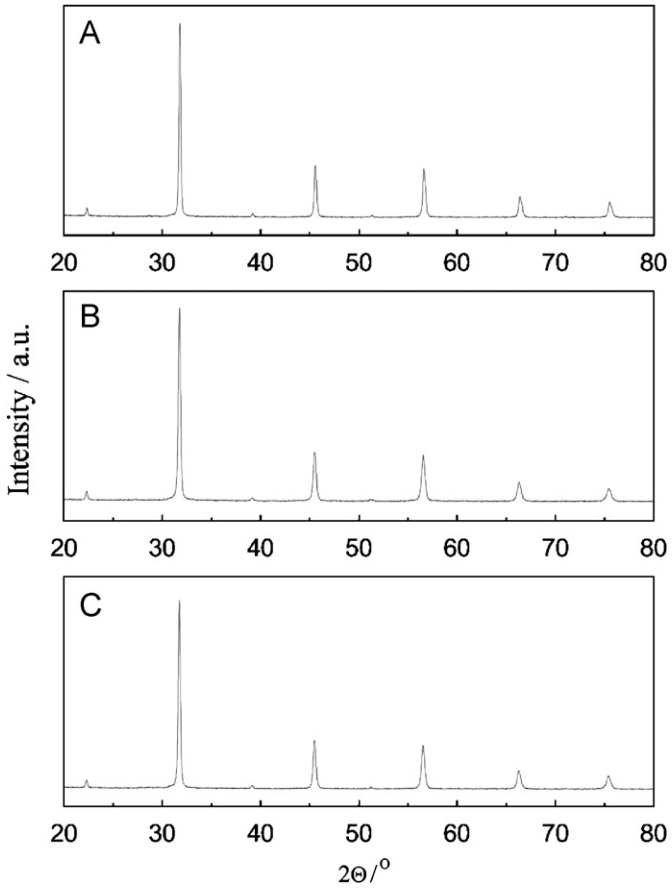

Fig. 2. XRD patterns of $SrMoO_4$ samples reacted with NH_3: (A) 11 h reacted sample, (B) 48 h reacted sample, and (C) 72 h reacted sample.

The dependence of the measured lattice constant from the nitrogen content of the samples is shown in Fig. 3. The lattice parameter of the sample treated for 11 h is 3.9782(1) Å, which is higher of that reported in the literature for $SrMoO_{2.5}N_{0.5}$ (3.9773(1) Å) [6] and of $SrMoO_3$. Larger lattice constants were found for the samples with higher nitrogen content. Nitrogen insertion is expected to lead to an increase of the cell parameter since the effective ionic radius of N^{3-} (1.32 Å) is larger than that of O^{2-} (1.26 Å). On the other hand, oxidation of Mo^{4+} (0.79 Å) to Mo^{5+} (0.75 Å) and Mo^{6+} (0.73 Å) [12,13] should lead to a decrease of the lattice constant. Although these two factors are expected to partly compensate each other, an increase of the lattice constant with the nitrogen content is measured, indicating that the influence of the larger anionic radius is the dominating effect.

Perovskite-type compounds often possess pseudosymmetry which originates from a tilting of the BO_6-octahedra, while the cations occupy the same positions as in the cubic aristotype structure. When the tilting is rather small it cannot be probed by XRD due to a low X-ray scattering power of anions. In contrast, the neutron scattering lengths of oxygen and nitrogen are large and therefore superstructure reflections, which occur due to the pseudosymmetry are often intense. One example for such pseudosymmetry is $SrNbO_2N$, which, according to XRD, crystallizes as a simple cubic perovskite while ND revealed a tetragonal supercell [14]. Additionally, since oxygen and nitrogen are distinguishable with neutrons, ND allows to verify the O/N content measured by hotgas extraction.

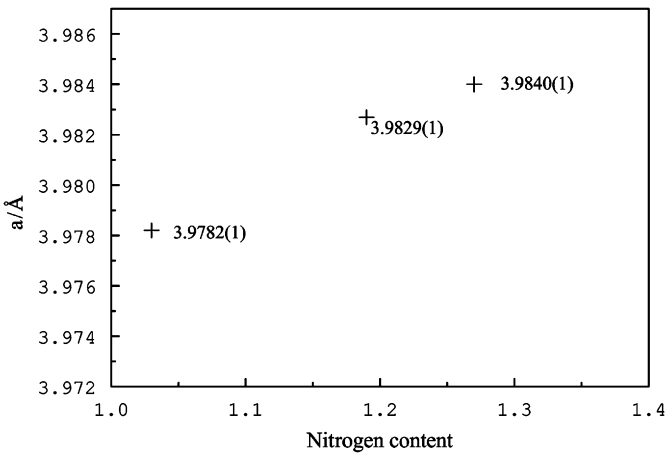

Fig. 3. The influence of the nitrogen content (measured by hotgas extraction) on the lattice constants (refined from XRD data) of the samples.

Rietveld refinement of the 11 h ammonolysed sample was carried out in the space group $Pm\bar{3}m$. In the starting structural model the Sr:Mo ratio was set to 1:1 (based on the cationic compositions study), whereas the O:N ratio was set to 2:1. Thermal displacement factors were refined isotropically for all atoms. The occupancy factors for oxygen and nitrogen were initially refined with the anionic site constrained to be fully occupied. In succeeding runs the occupancy factors of the anions were refined independently. Finally, the lattice and the profile parameters, $2\Theta_0$, the background coefficients, the thermal displacement factors and the anionic occupancies were refined together. Within the doubled standard deviation (2σ) no difference between the parameters obtained with the constrained and the unconstrained model were found. For this reason in the final refinement a complete occupation of the anionic sites was assumed and only the O/N ratio was refined. Refinements of cationic occupancies gave no hints for the presence of the cationic vacancies. A summary of the structural parameters refined from the neutron data can be found in Table 1. The statistics of the refinement, the visual inspection of the fit (Fig. 4) and the refined values of the thermal displacement factors indicate that the chosen model is correct. The refined O/N content corresponds to the composition $SrMoO_{1.89(2)}N_{1.11(2)}$, which is in a reasonable agreement with the result obtained by hotgas extraction.

Table 1
Structural parameters of the $SrMoO_{1.95}N_{1.05}$ refined from neutron powder data

Name	x	y	z	B_{iso} (Å^2)	Occupancy factor	Site
Sr	1/2	1/2	1/2	0.92(4)	1	1*b*
Mo	0	0	0	0.72(4)	1	1*a*
O/N(1)	1/2	0	0	0.64(2)	0.64(1)/0.36(1)	3*d*

Space group: $Pm\bar{3}m$ ($a = 3.9835(1)$ Å, $wR_p = 6.78$, $R_p = 5.20$, $\chi^2 = 1.36$).

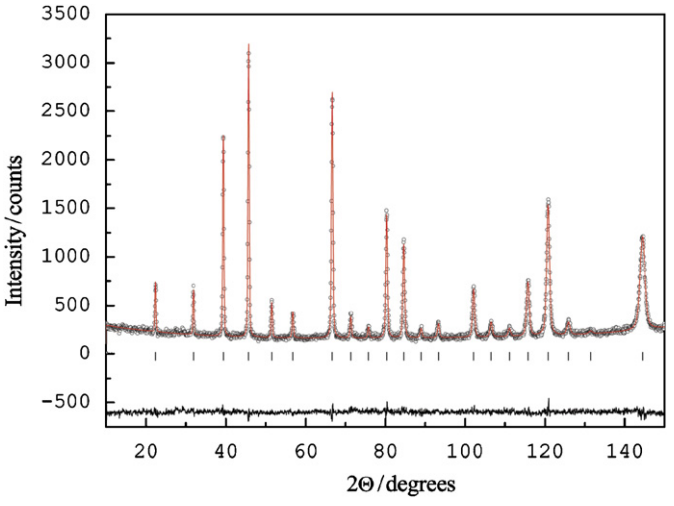

Fig. 4. Rietveld refinement plot of the ND data for the 11 h ammonolyzed sample. Space group: $Pm\bar{3}m$, $a = 3.9835(1)$ Å, $wR_p = 6.78$, $R_p = 5.20$, $\chi^2 = 1.36$.

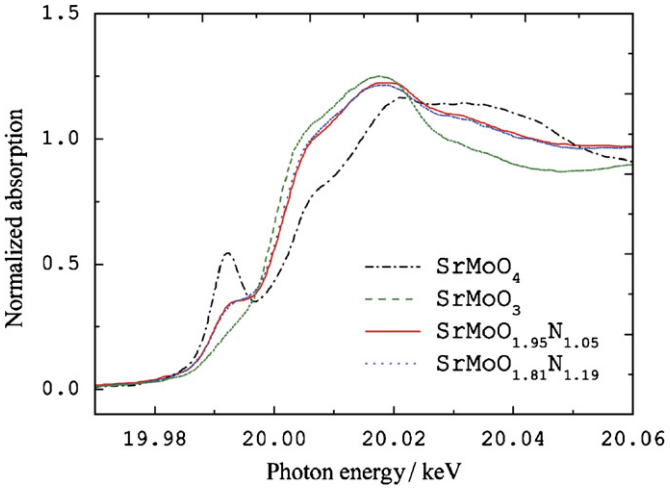

Fig. 5. Normalized Mo*K*-edge XANES spectra of the oxynitrides in comparison to the $SrMoO_3$ and $SrMoO_4$ standards.

The Mo*K*-edge XANES spectra of $SrMoO_3$, $SrMoO_4$, $SrMoO_{1.95(5)}N_{1.05(5)}$ and $SrMoO_{1.81(5)}N_{1.19(5)}$, are shown in Fig. 5. The edge shifts are obtained by using a well resolved feature above the absorption edge as shown in the inset of Fig. 5, and are reported relative to the first inflection point in the Mo metal *K*-edge at 19.999 keV [15]. The shift of the Mo*K* absorption edge to higher phonon energies with respect to the metal standard gives information about the average valence of the Mo while the pre-edge features correspond to its coordination geometry [16].

The XANES spectrum of $SrMoO_4$ shows a strong pre-edge peak which arises from an allowed 1*s*–4*d* electronic transition for tetrahedral symmetry [17]. This characteristic can also be observed as a shoulder for the oxynitrides with compositions $SrMoO_{1.95(5)}N_{1.05(5)}$ and $SrMoO_{1.81(5)}N_{1.19(5)}$. Since no $SrMoO_4$ impurity was detected with XRD and ND, the feature most probably corresponds to a distortion in the octahedral oxygen environment of Mo-ions reported before for MoO_3 [16]. In the XANES spectrum of $SrMoO_3$, where Mo is in a regular octahedron, this feature is not observed. Since for the oxynitrides no deviations from the cubic symmetry and no anomalous displacement parameters of their constituent ions have been detected by using ND (see Table 1), the local distortions in the surrounding of the Mo ions must have a too small coherence length to be detected with diffraction techniques. Most probably, the symmetry reduction arises from the different polarizabilities of O^{2-} and N^{3-}-ions, and their disordered arrangement around the Mo-ions. This interpretation is in accordance with recent EXAFS studies on $BaTaO_2N$, which reveal distorted octahedral arrangement of the Ta^{5+}-ions [18]. It should be noted that like in our case neither XRD nor ND had given any hints on the possible deviation of the local symmetry from O_h. While diffraction methods give information on a long range ordering averaged over the whole sample, XAS

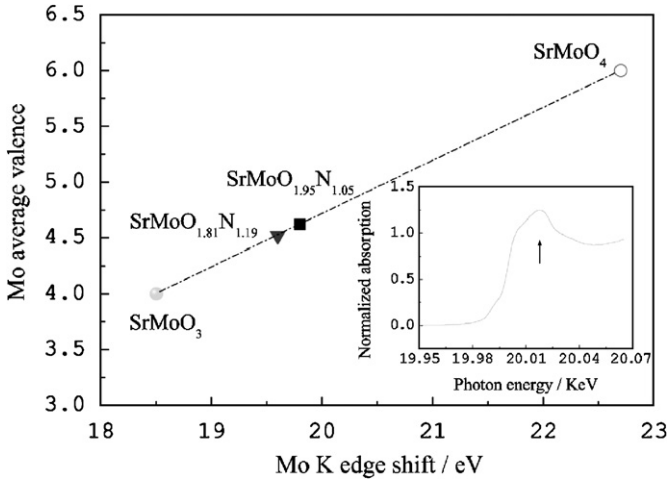

Fig. 6. Linear relationship of average Mo valence and Mo*K*-edge position (relative to Mo metal) calculated from *K*-edge position of the standards $SrMoO_3$ and $SrMoO_4$.

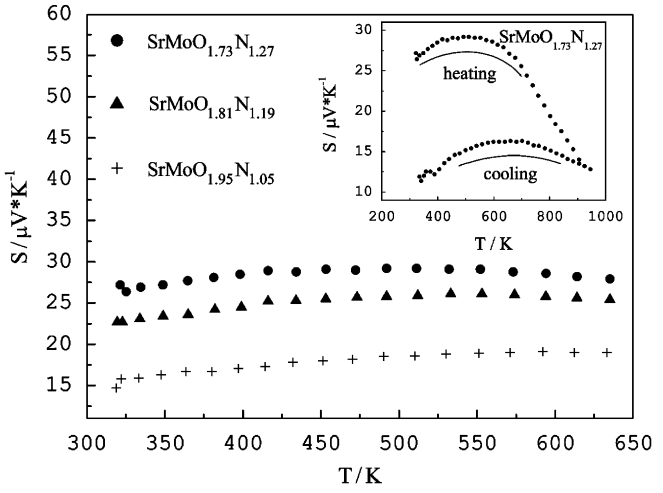

Fig. 7. Temperature dependence of Seebeck coefficient of the oxynitrides. The inset shows an irreversible decrease of the measured values when samples were heated above their decomposition temperature.

is sensitive to the short-range surrounding of the respective element and therefore this method is well suited to detect local deviations from the average symmetry [19].

From the energy shift of the X-ray absorption edge, the oxidation state of transition metals can be derived [20]. Fig. 6 depicts the calculated average Mo valence state for $SrMoO_{1.95(5)}N_{1.05(5)}$ (+4.62) and $SrMoO_{1.81(5)}N_{1.19(5)}$ (+4.52). On the other hand, the valence state obtained from the O/N content of these samples are +5.03 for $SrMoO_{1.95(5)}N_{1.05(5)}$ and +5.19 for $SrMoO_{1.81(5)}N_{1.19(5)}$. This seeming discrepancy can be explained by the fact that the absorption edge shift originates from both the "valence shift" (i.e. shift due to changing the oxidation state) and the "chemical shift" (shift due to different electronegativities of O^{2-} and N^{3-}-ligands). Since the oxide standards used are not able to account for differences in electronegativity of the anions, a big discrepancy between the calculated and the expected Mo valences arises.

The measured Seebeck coefficient values for the synthesized samples are up to three times higher than those reported for $SrMoO_3$ ($S = 4$–$9\,\mu V/K$) [7] but still close to those of metals. The Seebeck coefficient increases with increasing nitrogen content of the samples. The evolution of S with temperature and N content is shown in Fig. 7. Apparently, the values for all samples increase with temperature passing through a maximum at $T = 650\,K$ for $SrMoO_{1.95}N_{1.05}$, $T = 600\,K$ for $SrMoO_{1.81}N_{1.19}$ and $T = 550\,K$ for $SrMoO_{1.73}N_{1.27}$. Further heating of the samples is leading to the formation of metallic Mo impurity phase as revealed by XRD and an irreversible decrease of the Seebeck coefficient. Thus, the temperature at which the maximum of the Seebeck is reached can be considered as decomposition temperature. Apparently, the formation of metallic Mo is coupled with a nitrogen release from the samples. We have already reported similar behavior for Ca-substituted $LaTiO_2N$ heated under N_2 (1 atm) [8]. The main driving force for the reduction

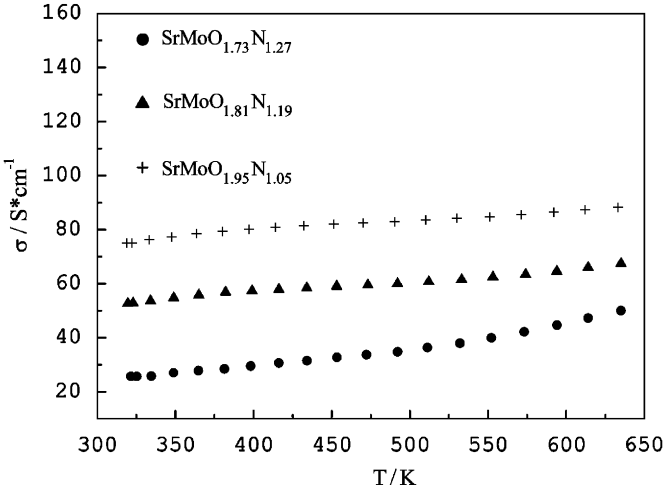

Fig. 8. Temperature dependence of electrical conductivity of the oxynitrides.

of Mo is the formation of the very stable N_2 molecule (941 kJ/mol).

The electrical conductivity of the samples decreases with increasing nitrogen content as shown in Fig. 8. Contrary to the metallic $SrMoO_3$ the electrical conductivity of the oxynitrides increases with temperature, i.e. a semiconducting behavior is observed. The measured conductivity values are 3 orders of magnitude lower than those of $SrMoO_3$ ($12.8 \times 10^3\,S\,cm^{-1}$) [7] and are of the same order of magnitude as those of $SrMoO_{2.6}N_{0.4}$ ($66.7\,S\,cm^{-1}$) [5], but one order of magnitude higher than reported for $SrMoO_{2.5}N_{0.5}$ ($2\,S\,cm^{-1}$) [6]. It should also be noticed that the temperature dependence of the $SrMoO_{2.6}N_{0.4}$ conductivity is semiconductor-like [5] similar to our samples, whereas that of $SrMoO_{2.5}N_{0.5}$ was described as metallic [6].

The power factor of our samples increases with temperature (Fig. 9). The measured values are lower than

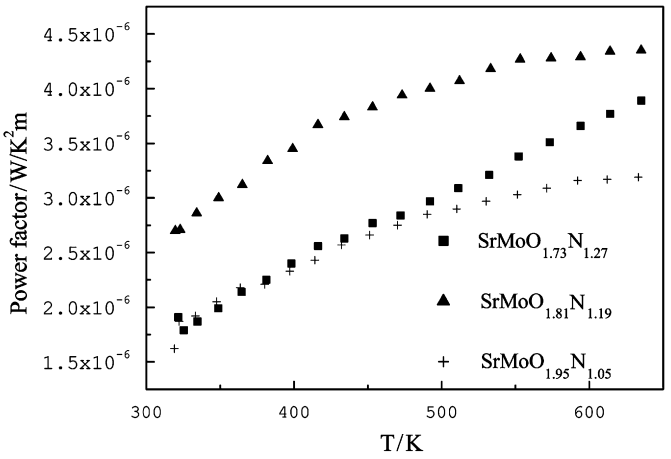

Fig. 9. Variation of power factor of the oxynitrides samples with temperature.

those reported for $SrMoO_3$ [21] due to the lower electrical conductivity of the oxynitrides.

The conductivity values and behavior of our samples are typical for semiconductors or poor metals. The density achieved for the ceramics (up to 89% of the theoretical density) resembles the one reported for $SrMoO_3$ (90.8%) [7]. The observed high deviation between the conductivity values measured on our samples and reported for $SrMoO_3$ therefore cannot be attributed to the difference between the samples density. Another factor that can affect the conductivity and its temperature dependence is the composition of grain boundaries. Indeed, taking into account that the samples are air sensitive, it may happen that the grain surface partly reoxidizes during the handling and the measured slight temperature dependence of the conductivity originates from the grain boundaries influence. The measured Seebeck values suggest that the synthesized samples are metallic-like. To clarify, whether the measured semiconductive behavior of the conductivity is an intrinsic property of our samples further investigations are in progress. In particular, thin films resistivity measurements free from grain boundaries effects can help to verify the conductivity values obtained in present study.

4. Conclusions

Solid solutions of the general composition $SrMoO_{3-x}N_x$ with $x>1$ were successfully synthesized by thermal ammonolysis of $SrMoO_4$. The nitrogen content of our samples is more than twice higher than previously reported and is confirmed by both ND and hotgas extraction. XANES studies result in a lower oxidation state of Mo with respect to the values calculated from the nitrogen content, resulting from a higher covalency of the Mo–N bond compared to the Mo–O bond ("chemical shift"). Both XRD and ND reveal no deviations from the cubic perovskite structure for the synthesized compounds, whereas local distortions of the $Mo(O,N)_6$ octahedra are detected with XANES. These distortions may arise due to the different polarizabilities of O^{2-} and N^{3-} and anionic disorder. Seebeck values of the oxynitrides are similar to those of metals. Smaller values of electrical conductivity of our samples compared to those of $SrMoO_3$ are measured. Electrical transport property measurements on single crystalline thin films with the same compositions are planned for the future to study the possible influences of grain boundaries on the physical properties.

Acknowledgments

The authors acknowledge the German Science Foundation (DFG-SPP 1136), Swiss Science Foundation (SNF-MaNEP) and Empa for the financial support as well as Dr. Denis Sheptyakov (SINQ) for the technical assistance. This work is partly based on the experiments performed at the Swiss Spallation Neutron Source SINQ, Paul Scherrer Institute, Villigen, Switzerland.

References

[1] P. Antoine, R. Assabaa, P. L'Haridon, R. Marchand, Y. Laurent, C. Michel, B. Raveau, Mater. Sci. Eng. B 5 (1989) 43–46.
[2] P. Antoine, R. Marchand, Y. Laurent, C. Michel, B. Raveau, Mater. Res. Bull. 23 (1988) 953–957.
[3] P. Dougier, A. Casalot, J. Solid State Chem. 2 (1970) 396–403.
[4] P. Dougier, P. Hagenmuller, J. Solid State Chem. 15 (1975) 158–166.
[5] G. Liu, X. Zhao, H.A. Eick, J. Alloys Compd. 187 (1992) 145–156.
[6] I.D. Fawcett, K.V. Ramanujachary, M. Greenblatt, Mater. Res. Bull. 32 (1997) 1565–1570.
[7] L.H. Brixner, J. Inorg. Nucl. Chem. 14 (1960) 225–230.
[8] D. Logvinovich, A. Börger, M. Döbeli, S.G. Ebbinghaus, A. Reller, A. Weidenkaff, Prog. Solid State Chem. 35 (2007) 281–290.
[9] P. Fischer, G. Frey, M. Koch, M. Konnecke, V. Pomjakushin, J. Schefer, R. Thut, N. Schlumpf, R. Burge, U. Greuter, Physica B 276–278 (2000) 146–147.
[10] J. Rodriguez-Carvajal, Physica B 192 (1993) 55–69.
[11] T. Ressler, J. Synchrotron Rad. 5 (1998) 118–122.
[12] R.D. Shannon, C.T. Prewitt, Acta Crystallogr. B: Struct. Sci. 25 (1969) 925–946.
[13] R. Shannon, Acta Crystallogr. A: Found. Crystallogr. 32 (1976) 751–767.
[14] S.G. Ebbinghaus, A. Weidenkaff, A. Rachel, A. Reller, Acta Crystallogr. C: Cryst. Struct. Commun. 60 (2004) i91–i93.
[15] J.A. Bearden, A.F. Burr, Rev. Mod. Phys. 39 (1967) 125–142.
[16] T. Ressler, O. Timpe, T. Neisius, J. Find, G. Mestl, M. Dieterle, R. Schlogl, J. Catal. 191 (2000) 75–85.
[17] F.W. Kutzler, C.R. Natoli, D.K. Misemer, S. Doniach, K.O. Hodgson, J. Chem. Phys. 73 (1980) 3274–3288.
[18] B. Ravel, Y.-I. Kim, P.M. Woodward, C.M. Fang, Phys. Rev. B: Condens. Matter Mater. Phys. 73 (2006) 184121–184127.
[19] S.G. Ebbinghaus, A. Weidenkaff, R.J. Cava, J. Solid State Chem. 167 (2002) 126–136.
[20] S. Ebbinghaus, Z. Hu, A. Reller, J. Solid State Chem. 156 (2001) 194–202.
[21] T. Maekawa, K. Kurosaki, H. Muta, M. Uno, S. Yamanaka, J. Alloys Compd. 390 (2005) 314–317.